Journal of Nanoporous Systems

Original Research Paper

Engineering bio-derived nanoporous interfacial layers from *Cynodon dactylon* for corrosion mitigation of copper in chloride environments

Mohammad Mahdi Alemnezhad[1], Mehdi Hosseini*[1, 2], Faezeh Omidali[1]

[1] *Department of Chemistry, Faculty of Basic Sciences, Ayatollah Boroujerdi University, Boroujerd, Iran.*
[2] *Biosensor and Energy Research Center, Ayatollah Boroujerdi University, Boroujerd, Iran.*

Article history
Received: 28 May 2026
Revised: 8 July 2026
Accepted: 11 July 2026

*Corresponding Author:
Mehdi Hosseini, Department of Chemistry, Faculty of Basic Sciences, Ayatollah Boroujerdi University, Boroujerd, Iran;

Email:
Hosseini.mehdi@abru.ac.ir

Abstract: The corrosion inhibition performance of Cynodon dactylon aqueous extract (CDAE) toward copper in 3.5 wt.% NaCl solution was comprehensively investigated using electrochemical, surface, and thermodynamic approaches. The phytochemical composition of the extract was initially characterized by GC-MS analysis, revealing the presence of oxygen- and nitrogen-containing organic compounds capable of interacting with the copper surface. The anticorrosion behavior of CDAE was evaluated through potentiodynamic polarization (PDP) and electrochemical impedance spectroscopy (EIS) measurements at different inhibitor concentrations and temperatures. Electrochemical results demonstrated that CDAE acts as an effective mixed-type inhibitor, significantly reducing the corrosion current density and increasing the charge transfer resistance. The inhibition efficiency increased with inhibitor concentration and reached a maximum value of 91.63% at 300 mg L^{-1} according to EIS analysis. The decrease in double-layer capacitance confirmed the adsorption of inhibitor molecules and the engineering of a compact nanoporous bio-derived interfacial protective layer on the copper surface. SEM-EDS analyses further verified the substantial reduction in surface deterioration in the presence of CDAE. Temperature-dependent studies indicated that the inhibition efficiency decreases with increasing temperature, suggesting a predominantly physical adsorption mechanism. Thermodynamic parameters, including activation energy, enthalpy, and entropy, supported the spontaneous adsorption behavior and interfacial stabilization process of the inhibitor film. Overall, the findings demonstrate that CDAE is a highly efficient, eco-friendly, low-cost, and sustainable green inhibitor capable of promoting stable nanoporous protective interfacial layer formation for corrosion mitigation of copper in chloride-containing environments.

Keywords: Copper corrosion, green inhibitor, *Cynodon dactylon*, nanoporous interfacial layer, electrochemical impedance spectroscopy, potentiodynamic polarization, adsorption mechanism.

Introduction

Corrosion is a persistent and economically damaging phenomenon that severely affects the durability and reliability of metallic materials in industrial systems [1-3]. Among engineering metals, copper is widely utilized in marine structures, heat exchangers, desalination systems, electrical devices, and water transportation networks because of its excellent electrical conductivity, thermal stability, and mechanical processability [4,5]. However, chloride-containing environments significantly accelerate copper dissolution and induce localized corrosion phenomena such as pitting and crevice corrosion, thereby reducing the operational lifetime of copper-based infrastructures [6,7]. Consequently, the development of efficient and environmentally sustainable corrosion protection systems remains a major challenge in modern materials and surface engineering [8]. Traditional corrosion protection approaches, including alloying, polymer coatings, cathodic protection, and synthetic organic inhibitors, have shown acceptable inhibition performance under various aggressive conditions [9,10]. Nevertheless, many conventional inhibitors suffer from severe drawbacks such as toxicity, poor biodegradability,

environmental persistence, and high production cost [11]. These limitations have directed recent research toward the development of eco-friendly green inhibitors derived from renewable natural resources [12-14]. Plant-derived inhibitors have attracted substantial attention because they contain abundant heteroatom-rich phytochemicals such as flavonoids, alkaloids, tannins, terpenoids, and oxygenated aromatic compounds capable of adsorbing onto metallic surfaces and forming compact protective films [15-17]. In particular, aqueous plant extracts provide additional environmental advantages because water acts as a safe, inexpensive, and non-toxic extraction medium without requiring hazardous organic solvents [18]. The adsorption of these bioactive molecules on metallic surfaces can significantly reduce anodic metal dissolution and suppress cathodic reactions through interfacial barrier layer formation [19]. In recent years, corrosion science has increasingly benefited from concepts originally developed in separation chemistry, interfacial chemistry, and micro-scale extraction systems. In particular, ionic liquids and microextraction-based platforms have demonstrated that interfacial organization of organic cations/anions can strongly regulate mass transfer, adsorption behavior, and surface selectivity at solid–liquid interfaces. These principles are directly transferable to corrosion systems, where inhibition efficiency is fundamentally governed by adsorption strength and interfacial film stability. Ionic liquids have recently emerged as promising corrosion-protective media and interfacial modifiers owing to their tunable physicochemical properties, including adjustable hydrophobicity, high ionic density, negligible vapor pressure, and strong affinity for metallic surfaces. These unique characteristics enable ionic liquids to adsorb onto metal substrates, form protective interfacial films, and mitigate the aggressiveness of corrosive environments, thereby significantly enhancing corrosion resistance [20–22]. From a mechanistic perspective, the same driving forces that govern preconcentration and selective extraction of trace species in microextraction systems—such as electrostatic interaction, hydrogen bonding, and hydrophobic association—can also regulate the formation of protective adsorption layers on metal surfaces. In this context, task-specific ionic liquids and hydrophobic conversion-assisted systems have been shown to construct highly ordered interfacial architectures, which significantly enhance stability and resistance against aggressive media [23,24]. Our previous studies have demonstrated that engineered ionic liquid systems can effectively modulate interfacial behavior in both analytical and environmental applications, particularly in trace analysis, separation, and surface-assisted reaction environments [25-27]. These findings suggest that rational design of interfacial molecular systems can bridge the gap between analytical chemistry and corrosion science by enabling controlled adsorption and surface passivation processes [28]. Alongside synthetic interfacial systems, biomass-derived materials have emerged as promising sustainable alternatives for corrosion inhibition due to their natural abundance, low cost, and rich phytochemical composition [29]. However, the efficiency of such systems is highly dependent on their ability to form stable and compact interfacial films, which requires deeper understanding of adsorption thermodynamics and surface interaction mechanisms. In this context, Cynodon dactylon is particularly attractive because it is an abundant fast-growing weed widely distributed across agricultural lands and natural ecosystems in Iran, especially Lorestan province. Despite its wide availability, this biomass has minimal industrial value and is typically considered agricultural waste. Converting this neglected plant into a functional corrosion protection material not only adds value to waste biomass but also aligns with sustainable materials engineering principles [30,31]. Recently, considerable attention has been directed toward the development of environmentally friendly corrosion inhibitors based on natural plant extracts as sustainable alternatives to conventional toxic chemicals. Among these, *Cynodon dactylon* extract has shown excellent corrosion inhibition performance for mild steel in acidic media and has also been successfully incorporated into epoxy coating systems to enhance corrosion protection in aggressive environments. These findings highlight the significant potential of plant-derived phytochemicals as green corrosion inhibitors and protective coating additives for metallic materials [32,33].

In this study, copper was selected as the substrate of interest due to its extensive use in vital industrial equipment such as heat exchangers and cooling systems. Given its high susceptibility to corrosion in saline (chloride-rich) environments, protecting copper against degradation is an urgent technical and economic priority. Furthermore, copper serves as a benchmark material in electrochemical studies, allowing for a precise evaluation of the interfacial inhibition efficiency of the proposed green inhibitor.

In the present study, the corrosion inhibition behavior of aqueous extract of Cynodon dactylon toward copper in 3.5 wt.% NaCl solution was comprehensively investigated using electrochemical, thermodynamic, and surface analytical techniques. The phytochemical constituents of the extract were identified through GC-MS analysis, while inhibition performance was evaluated using linear sweep voltammetry (LSV) and electrochemical impedance

spectroscopy (EIS). Surface morphology and protective layer formation were examined using SEM-EDS analysis. Moreover, adsorption isotherm modeling and thermodynamic parameters including ΔH°, ΔS°, and activation energy were employed to elucidate the inhibition mechanism and adsorption behavior of the extract on the copper surface. Unlike conventional studies that mainly focus on inhibition efficiency, the present work emphasizes the interfacial engineering aspect of corrosion protection, where adsorption of oxygen- and nitrogen-containing phytochemicals leads to the formation of a compact, nanoporous-like protective layer on copper. In addition, the conceptual framework of ionic liquid-assisted interfacial control and micro-scale extraction chemistry is indirectly integrated to explain how molecular organization and surface affinity govern film stability and corrosion resistance. This multidisciplinary perspective connects green corrosion inhibition with interfacial chemistry principles widely used in separation science and microextraction systems.

Overall, the novelty of the present study lies in combining sustainable biomass utilization with interfacial physicochemical engineering concepts to develop a green, efficient, and mechanistically well-understood corrosion mitigation strategy for copper in chloride environments.

Materials and Methods

Chemicals

Copper specimens were employed as the metallic substrate in all corrosion experiments. Rectangular coupons of commercially pure copper were mechanically abraded using silicon carbide emery papers of progressively finer grit, followed by thorough rinsing with deionized water (DI), degreasing with ethanol, and drying in air. The corrosive medium consisted of a 3.5 wt.% NaCl aqueous solution prepared from analytical grade sodium chloride and DI water, and all solutions were freshly prepared prior to each set of measurements. Fresh *Cynodon dactylon* was collected from the *Borujerd* plains (desert areas), *Lorestan Province, Iran*. The plant material, regarded as an abundant, low value weed without significant industrial or commercial utilization, was carefully washed with tap water to remove adhering soil and impurities, subsequently rinsed with DI water, and dried at ambient temperature. The dried biomass was then ground to a fine powder. An aqueous extract of *Cynodon dactylon* (CDAE) was obtained by dispersing a known mass of the powdered material in DI water and subjecting the mixture to controlled heating under continuous stirring for a fixed duration. After cooling to room temperature, the suspension was filtered to remove solid residues, and the resulting filtrate was used as the CDAE stock solution. Test solutions containing different CDAE concentrations were prepared by appropriate dilution of the stock extract with 3.5 wt.% NaCl solution. Electrochemical measurements were conducted in a conventional three electrode glass cell, employing copper as the working electrode (WE), a platinum foil as the counter electrode (CE), and an Ag, AgCl electrode as the reference electrode (RE). Prior to each experiment, the WE was immersed in the test solution and allowed to reach a stable open circuit potential (OCP). Linear sweep voltammetry (LSV) was then used to obtain polarization curves for copper in the absence and presence of CDAE at various concentrations. Electrochemical impedance spectroscopy (EIS) was performed at OCP by applying a small amplitude sinusoidal perturbation over a suitable frequency range, and the resulting impedance spectra were analyzed by equivalent circuit (EC) fitting to extract the relevant electrochemical parameters. The chemical composition of CDAE was investigated by gas chromatography–mass spectrometry (GC-MS). For this purpose, the aqueous extract was concentrated and, where necessary, subjected to liquid–liquid extraction (LLE), followed by solvent removal and re dissolution in a volatile organic solvent compatible with GC-MS analysis. Chromatographic separation was achieved on a capillary column under a programmed oven temperature regime, and individual constituents were identified by comparison of their mass spectra with reference library databases. Surface morphology of copper specimens after exposure to the corrosive medium, in the absence and presence of CDAE, was examined by scanning electron microscopy (SEM) in order to provide visual evidence of surface damage and to assess the formation of a protective layer attributable to inhibitor adsorption. The adsorption behavior of CDAE on the copper surface was further evaluated by fitting the experimental inhibition data to common adsorption isotherm models, and the associated thermodynamic parameters, including the standard enthalpy and entropy of adsorption (ΔH^o and ΔS^o), were estimated to gain additional insight into the physicochemical nature of the adsorption process.

Analytical methodology

An aqueous extract of *Cynodon dactylon* (CDAE) was prepared by ultrasonic-assisted water extraction for subsequent anticorrosion evaluation. In brief, 4 g of the dried and finely powdered plant material was placed into a 200 mL flask, after which 100 mL deionized water (DI) was added. The mixture was subjected to ultrasonic extraction at 70°C for 25 min. The resulting suspension was filtered through Whatman filter paper (12.5 cm), and the obtained filtrate was used as the stock CDAE solution. Working solutions with different concentrations were prepared by dilution of the stock extract with the 3.5 wt.% NaCl solution.

To characterize the chemical composition and identify potential bioactive constituents, an ethanolic extract of *Cynodon dactylon* was prepared via the Soxhlet extraction method. This method was selected to ensure the efficient and exhaustive isolation of secondary metabolites. Specifically, analytical-grade ethanol was employed as the solvent due to its optimal suitability for the Soxhlet reflux process and its ability to effectively solubilize a broad spectrum of phytochemicals. A known mass of the powdered plant material was loaded into the Soxhlet chamber and extracted with 125 mL of ethanol at 90 °C for 24 h. Upon completion of the extraction, the solvent was evaporated under reduced pressure using a rotary evaporator. The resulting concentrated ethanolic extract was then stored in sealed vials for subsequent GC-MS analysis.

Results and Discussions

Throughout this study, the electrochemical parameters presented in the figures are defined as follows: E_{corr} and j_{corr} represent the corrosion potential and corrosion current density, respectively. In the electrochemical impedance spectroscopy (EIS) plots, Z and Z'' refer to the real and imaginary components of impedance, which are measured as a function of frequency (f). Furthermore, T denotes the experimental temperature expressed in Kelvin.

GC-MS analysis

Gas chromatography coupled with mass spectrometry was employed to elucidate the major organic constituents present in *Cynodon dactylon* ethanolic extract used for molecular characterization. The analyses were performed using an Agilent GC system (model 6890) equipped with an Agilent mass selective detector (model 5973). A fused-silica HP-5 capillary column with a film thickness of 0.25 µm was utilized. The oven program initiated at 45°C with a 1 min hold, followed by a temperature increase of 2°C. min^{-1} up to 200°C, where it was maintained for 30 min. The injector temperature was set at 220°C throughout the run. The identified compounds are summarized in Table 1. The chromatographic profile revealed the presence of diverse oxygenated and nitrogen-containing organic species, along with several minor components bearing heteroatoms capable of donating electron density. Functional groups such as alcohols, ketones, esters, and alkaloids were detected. These molecular features are known to enhance interaction with metallic surfaces by forming coordinate bonds with copper sites, thereby facilitating the development of an adsorbed protective film that contributes to corrosion inhibition in chloride-containing media.

Table 1. Major constituents identified in the ethanolic extract of *Cynodon dactylon* by GC-MS analysis.

Number	1	2	3	4	5
Name	2,3-Dihydro-benzofuran	Benzene acetic acid, α,4 hydroxy-3-methoxy-, methyl ester	Benzene methanol, 2,5 dimethyl-, acetate	Octadecanaldehyde	(2R,3S)-Butane-1,2,3,4-tetrol
Formula	C_8H_8O	$C_{10}H_{12}O_5$	$C_{10}H_{12}O_4$	$C_{18}H_{36}O$	$C_4H_{10}O_4$
2D structure	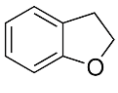	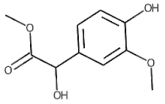	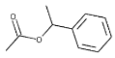	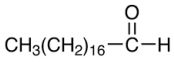	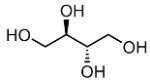

Electrochemical experiments

Electrochemical measurements, including potentiodynamic polarization (PDP) and electrochemical impedance spectroscopy (EIS), were conducted using a Potentiostat/Galvanostat system (Metrohm Autolab, PGSTAT 302N, Netherlands). A conventional three-electrode electrochemical cell was employed, consisting of a copper specimen as the working electrode (WE), a platinum rod as the counter electrode (CE), and an Ag/AgCl (3 M KCl) electrode as the reference electrode (RE). All tests were performed in a 3.5 wt.% NaCl solution in the absence and presence of various concentrations of CDAE (50-300 mg/L) at 298 K. Prior to each measurement, the WE was immersed in the electrolyte for 60 min to reach a stable open circuit potential (OCP). The PDP curves were recorded by scanning the potential from -250 to +250 mV versus OCP

at a constant scan rate of 1 mV. s^{-1}. The corrosion inhibition efficiency ($IE_{PDP}\%$ was determined using the following equation:

$$IE_{PDP}\% = \frac{j^{\circ}_{corr} - j_{corr}}{j^{\circ}_{corr}} \times 100 \quad (1)$$

where j°_{corr} and j_{corr} represent the corrosion current density values in the absence and presence of CDAE, respectively.

EIS experiments were performed at the OCP within a frequency range of 10^5 Hz to 10^{-1} Hz, using a sinusoidal potential amplitude of 10 mV. The inhibition efficiency from the EIS data ($IE_{EIS}\%$) was calculated as follows:

$$IE_{EIS}\% = \frac{R_{CT} - R^{\circ}_{ct}}{R_{CT}} \times 100 \quad (2)$$

where R_{CT} and R°_{ct} are the charge transfer resistance values in the presence and absence of the inhibitor, respectively. All electrochemical tests were performed in triplicate to ensure the reproducibility of the results.

Polarization study

Potentiodynamic polarization curves obtained for copper in 3.5 wt.% NaCl containing different concentrations of CDAE are presented in Figure 1. These curves provide key electrochemical parameters such as corrosion potential (E_{corr}), anodic and cathodic Tafel slopes (β_a and β_c), and corrosion current density (j_{corr}), which were extracted through Tafel extrapolation and summarized in Table 2. The polarization results show a clear reduction in j_{corr} upon the addition of CDAE, and this reduction becomes progressively more significant as the concentration increases from 50 to 300 mg. L^{-1}. This trend indicates that CDAE effectively decreases the corrosion rate by forming a protective layer over the copper surface and by hindering both anodic metal dissolution and cathodic oxygen reduction reactions. A slight positive shift in E_{corr} was also observed in the presence of CDAE. However, the magnitude of this shift remained below the commonly accepted threshold that distinguishes anodic- or cathodic-dominant inhibitors. Therefore, the overall behavior suggests that CDAE functions as a mixed-type inhibitor, exerting simultaneous influence on both reaction pathways without strongly favoring either. Additionally, although higher concentrations of CDAE consistently improved the inhibition performance, the increase in efficiency between 200 and 300 mg. L^{-1} became less pronounced. This diminishing improvement at elevated concentrations implies that the copper surface gradually approaches saturation with the active molecules of CDAE. Based on this trend, 300 mg. L^{-1} represents a practical upper level for effective inhibition while maintaining reasonable inhibitor usage for subsequent studies.

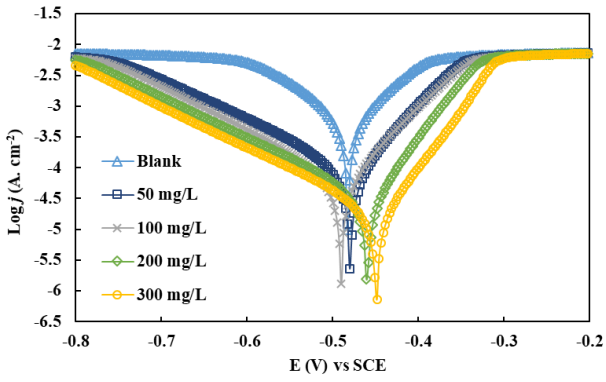

Fig. 1. Polarization curves of copper in 3.5 wt.% NaCl solution containing various CDAE concentrations at 298 K.

Table 2. Electrochemical polarization parameters for copper in 3.5 wt.% NaCl in the absence and presence of different concentrations of CDAE at 298 K.

CDAE Conc. (mg. L^{-1})	E_{corr} (mV)	j_{corr} (μA.cm^{-2})	$-\beta_c$ (mV.dec^{-1})	$-\beta_a$ (mV.dec^{-1})	IE (%)
0	-256	24.8	142	118	–
50	-243	7.1	137	112	71.4
100	-238	5.6	133	109	77.4
200	-228	3.9	128	104	84.1
300	-219	2.8	122	101	88.5

The electrochemical degradation of copper in NaCl media proceeds through a series of synchronized anodic and cathodic processes. The cathodic reaction, associated with the reduction of dissolved oxygen, is represented as (Eq. 3):

$$O_2 + 2H_2O + 4\bar{e} \rightarrow 4OH^- \quad (3)$$

Simultaneously, the anodic dissolution of copper in chloride-containing electrolytes involves a multi-stage mechanism governed by the interaction with Cl^- ions:

$$Cu_{(s)} \rightarrow Cu^+_{(aq)} + \bar{e} \quad (4)$$
$$Cu_{(s)} + Cl^-_{(aq)} \rightarrow CuCl_{(insoluble)} + \bar{e} \quad (5)$$
$$CuCl_{(insoluble)} + Cl^-_{(aq)} \rightarrow [CuCl_2]^-_{(aq)} \quad (6)$$
$$[CuCl_2]^-_{(aq)} \rightarrow Cu^{2+}_{(aq)} + 2Cl^-_{(aq)} + \bar{e} \quad (7)$$

Firstly, copper atoms at the metal surface undergo oxidation to Cu^+ (Eq. 4). The subsequent reaction with chloride ions facilitates the formation of a semi-protective *CuCl* film on the interface (Eq. 5), which acts as a kinetic barrier, inducing a temporary reduction

in current density. However, due to the limited stability of this layer, it tends to transform into a soluble $[CuCl_2]^-$ complex (Eq. 6). Finally, this complex migrates into the bulk electrolyte, further dissociating into Cu^{2+} ions (Eq. 7), a process that leads to accelerated metal dissolution and an increase in current density. The addition of CDAE introduces organic molecules characterized by heteroatoms (such as O and N) and various phytochemicals. These molecules effectively mitigate the aforementioned anodic and cathodic reactions. The inhibition mechanism is attributed to the spontaneous adsorption of these molecules onto the copper surface, creating a robust, hydrophobic protective film. This adsorbed layer serves as a physical and chemical barrier that blocks the active sites, thereby preventing the diffusion of aggressive Cl^- ions toward the metal surface and suppressing both the cathodic oxygen reduction and the anodic dissolution of copper.

EIS measurements

Electrochemical impedance spectroscopy (EIS) results for copper in 3.5 wt.% NaCl, both in the absence and presence of various CDAE concentrations (50–300 mg. L^{-1}), are shown in Figure 2. The Nyquist and Bode plots clearly illustrate the change in electrochemical behavior upon inhibitor addition. To analyze these spectra, an equivalent electrical circuit (EEC) model consisting of $R_s(R_{ct}\ Q_{dl})$ was employed, where R_s represents the electrolyte resistance, R_{ct} is the charge transfer resistance, and Q_{dl} is the constant phase element (CPE) representing the electric double layer. The use of CPE instead of an ideal capacitor account for the surface inhomogeneity and non-ideal capacitive response of the copper electrode. The double layer capacitance C_{dl} was computed using the following relationship:

$$C_{dl} = Y_0(2\,\pi\,f_{max})^{n-1} \quad (8)$$

where Y_0 and f_{max} denote the CPE magnitude and the frequency at which the imaginary impedance component is maximized, respectively.

The electrochemical impedance spectroscopy (EIS) results for copper in 3.5 wt.% NaCl, in the absence and presence of CDAE (50-300 mg. L^{-1}), are presented in Table 3. As the inhibitor concentration increases, the diameter of the capacitive semicircles in the Nyquist plots increases significantly, which reflects an increase in charge transfer resistance R_{ct}, rising from 1.05 kΩ. cm^{-2} in the blank solution to 12.55 kΩ. cm^{-2} at 300 mg L^{-1}. The double layer capacitance C_{dl} values show a progressive decrease from 82.35 to 1.32 μF. cm^{-2}. This downward trend in C_{dl} is attributed to the replacement of water molecules (with a high dielectric constant) by organic inhibitor molecules (with a lower dielectric constant) at the metal-electrolyte interface, which confirms the formation of a protective adsorption layer on the copper surface. As CDAE concentration increases, the diameter of the capacitive semicircles in the Nyquist plots expands significantly, indicating a substantial increase in R_{ct} and a corresponding decrease in the corrosion rate. This enhancement in R_{ct} is consistent with the polarization results, reinforcing the efficiency of CDAE as a corrosion inhibitor. The observation of a single capacitive loop suggests that the corrosion process is predominantly controlled by a single charge transfer mechanism, with the CDAE molecules effectively forming a stable layer over the copper surface. Table 3 summarizes the fitted impedance parameters. A notable reduction in C_{dl} values with increasing CDAE concentration is observed, which can be attributed to a decrease in the local dielectric constant and/or an increase in the thickness of the electrical double layer. This phenomenon is indicative of the replacement of water molecules adsorbed on the copper surface by CDAE molecules, as described by the following displacement and adsorption mechanism:

$$\text{CDAE}_{(sol)} + n\text{H}_2\text{O}_{(ads)} \leftrightarrow \text{CDAE}_{(ads)} + n\text{H}_2\text{O}_{(sol)} \quad (9)$$

$$\text{Cu} + \text{CDAE}_{(ads)} \leftrightarrow [\text{Cu - Inhibitor}]_{(ads)} \quad (10)$$

These processes facilitate the formation of a dense, protective film that isolates the metal surface from the aggressive chloride ions in the environment, thereby providing efficient corrosion protection.

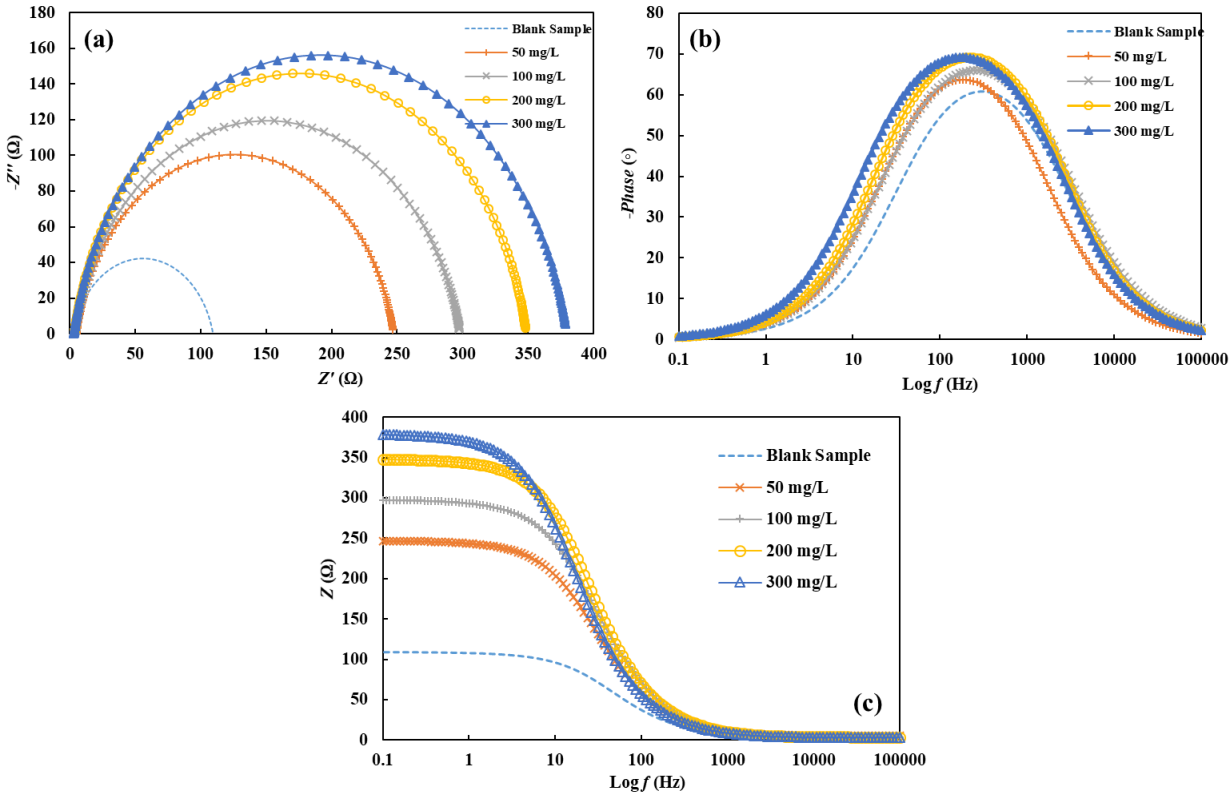

Fig. 2. Nyquist (a) and Bode (b and c) plots for copper in 3.5 % NaCl solution with different concentrations of CDAE.

Table 3. Impedance parameters obtained from EIS measurements for copper in 3.5 wt.% NaCl solution in the absence and presence of different concentrations of CDAE.

CDAE (mg. L^{-1})	f_{max} (Hz)	R_s ($\Omega.cm^2$)	R_p ($k\Omega.cm^2$)	CPE ($\mu Mho.s^n$)	n	C_{dl} ($\mu F.cm^2$)	IE%
0	0.224	4.10	1.05	242.0	0.582	82.35	----
50	0.751	3.38	3.48	34.8	0.731	8.17	69.83
100	2.085	3.25	5.82	8.21	0.788	1.85	81.96
200	1.892	3.35	6.75	7.15	0.815	1.68	84.44
300	1.285	3.18	12.55	5.42	0.808	1.32	91.63

SEM-EDS analysis

To evaluate the changes in surface morphology and elemental composition of the copper samples under different exposure conditions, SEM–EDS analysis was performed using a TESCAN VEGA/II SEM instrument equipped with an EDS detector. The copper surfaces were examined before immersion and after exposure to 3.5 wt.% NaCl solution for 1 and 24 h, both in the absence and presence of CDAE as the corrosion inhibitor. The corresponding SEM micrographs are presented in Figure 3, where each panel clearly represents a specific surface condition: polished copper before exposure, copper exposed to the uninhibited NaCl solution, and copper exposed to the CDAE-containing NaCl solution at the selected immersion times.

As shown in Figure 3, the polished copper surface exhibits a relatively smooth morphology before exposure to the corrosive medium. After immersion in the blank 3.5 wt.% NaCl solution, visible surface degradation appears, including dark corroded regions and surface irregularities. These features become more pronounced with increasing exposure time from 1 to 24 h, indicating progressive corrosion damage in the chloride-containing medium. In contrast, the copper samples exposed to the CDAE-containing solution show a considerably less damaged surface morphology. The dark corroded areas are markedly reduced, even after 24 h of immersion, suggesting that CDAE forms a protective interfacial layer that limits the direct contact between chloride ions and the copper surface.

The corresponding EDS spectra are shown in Figure 4 and provide further evidence of the surface changes induced by corrosion and inhibitor adsorption. The spectra obtained from the copper samples before and after immersion mainly show the characteristic signals of copper and oxygen. For the uninhibited samples, the decrease in the relative copper signal and the appearance/intensification of oxygen-related signals indicate the formation of corrosion products on the copper surface. However, in the presence of CDAE, the atomic percentage of copper remains higher than that observed for the uninhibited samples under the same exposure time. This result indicates that the CDAE layer suppresses copper dissolution and reduces the accumulation of corrosion products on the surface. Therefore, the SEM and EDS observations support the electrochemical results and confirm that CDAE effectively mitigates copper corrosion in 3.5 wt.% NaCl solution by forming a thin protective adsorbed layer on the metal surface.

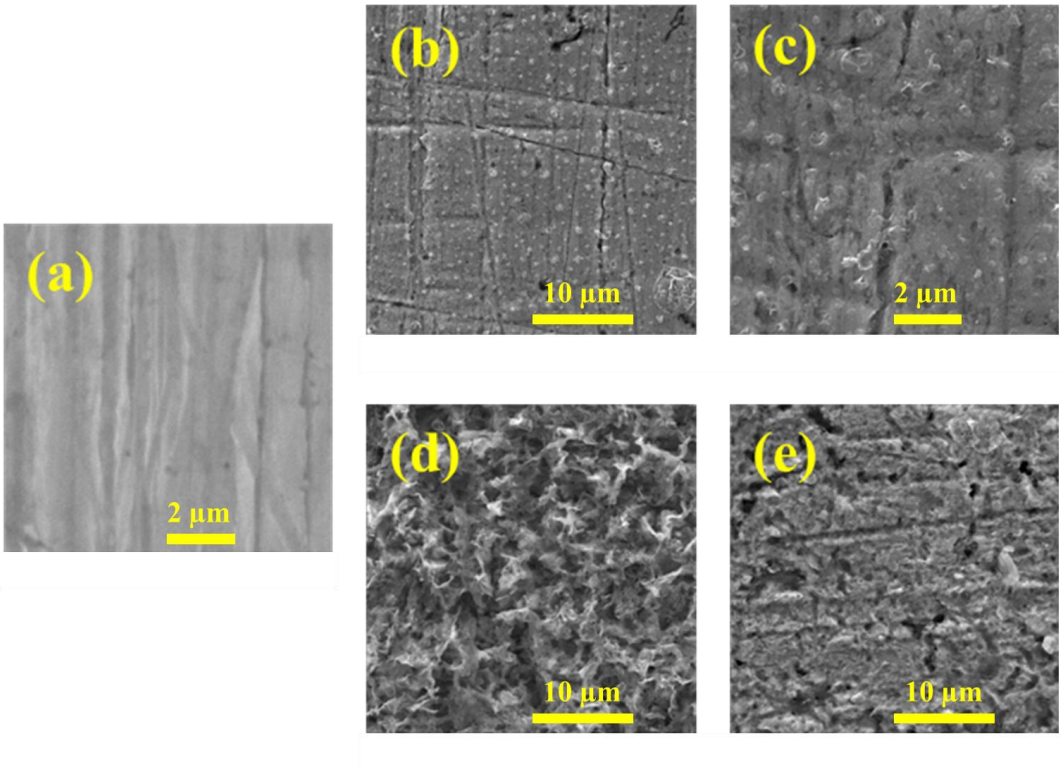

Fig. 3. SEM images of the copper surface: (a) polished copper before exposure to 3.5 wt.% NaCl solution, (b) after 1 h exposure to 3.5 wt.% NaCl solution without inhibitor, (c) after 1 h exposure to 3.5 wt.% NaCl solution with CDAE, (d) after 24 h exposure to 3.5 wt.% NaCl solution without inhibitor, and (e) after 24 h exposure to 3.5 wt.% NaCl solution with CDAE.

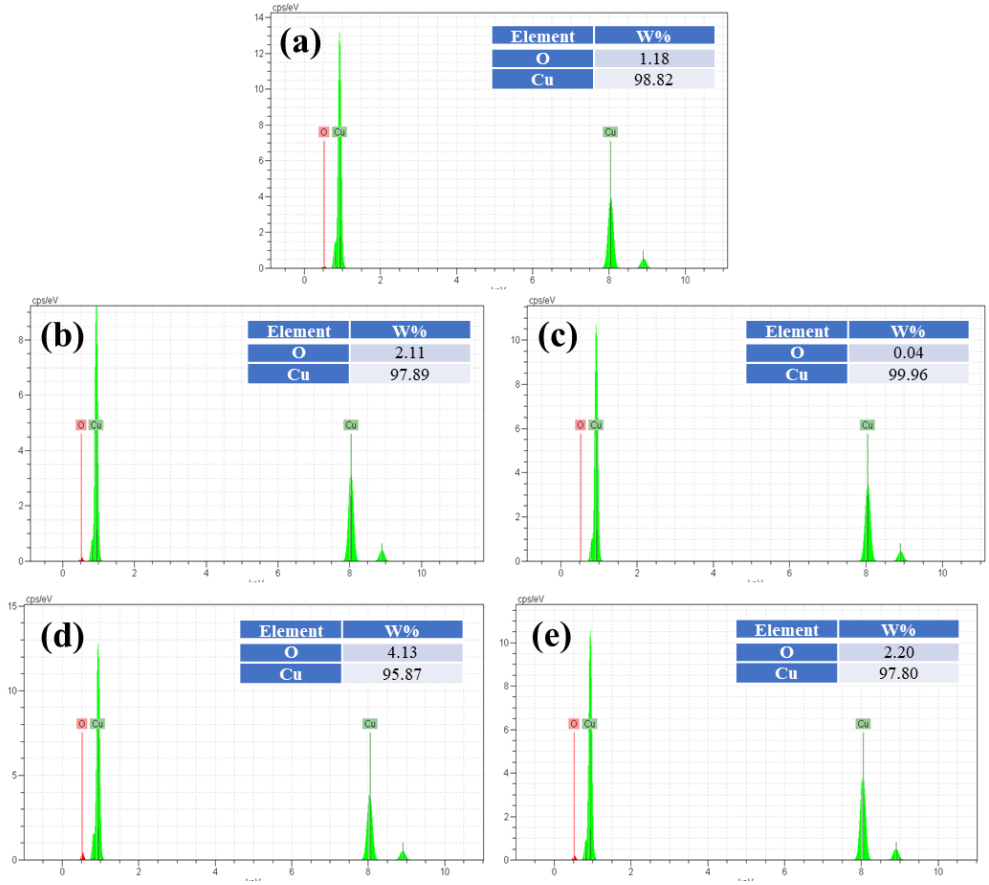

Fig. 4. EDS spectra of the copper surface: (a) polished copper before exposure to 3.5 wt.% NaCl solution, (b) after 1 h exposure to 3.5 wt.% NaCl solution without inhibitor, (c) after 1 h exposure to 3.5 wt.% NaCl solution with CDAE, (d) after 24 h exposure to 3.5 wt.% NaCl solution without inhibitor, and (e) after 24 h exposure to 3.5 wt.% NaCl solution with CDAE.

Effect of temperature

The temperature effect on the corrosion rate of alloys is undeniable, therefore, polarization measurements were conducted within the temperature range of 298 to 338 K, both in the absence and presence of 200 mg. L^{-1} of CDAE as the optimum inhibitor concentration. Figure 5 represents the polarization curves at different temperatures with a scan rate of 5 mV. s^{-1} in 3.5 wt.% NaCl solution, both with and without the optimum concentration of CDAE. A summary of the key polarization parameters is presented in Table 3. It is evident that an increase in temperature leads to a transition of E_{corr} values toward more negative potentials and an increment in j_{corr} values in both corrosive media, indicating that the corrosion rate of copper in 3.5 wt.% NaCl increases with temperature. According to Table 3, the increment of j_{corr} is less pronounced in the presence of the inhibitor compared to its absence. Furthermore, the inhibition efficiency (*IE%*) decreases as the temperature rises, suggesting that the surface coverage is reduced due to the desorption of inhibitor molecules from the copper surface. This thermal desorption facilitates the faster transition of the unstable *CuCl* layer into $[CuCl_2]_{(aq)}$ species.

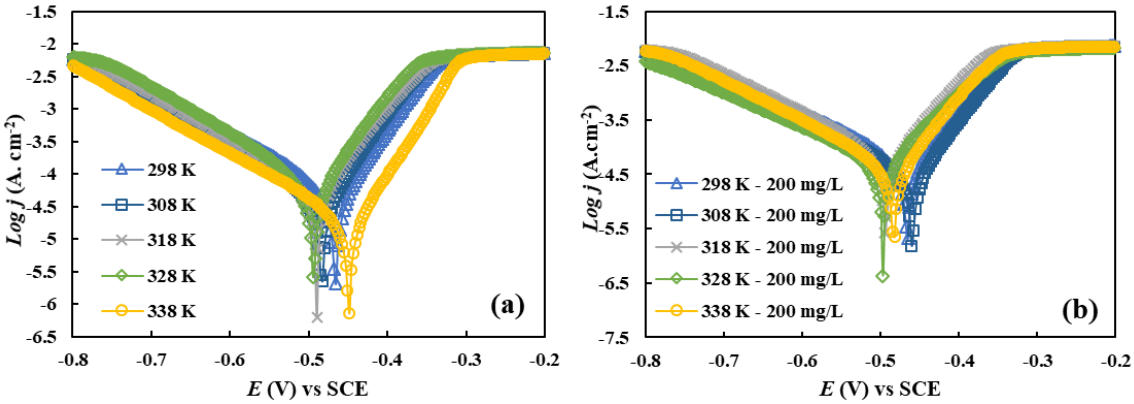

Fig. 5. Effect of temperature on polarization curves of copper in 3.5 wt.% NaCl solution in the absence (a) and presence (b) of 200 mg. L^{-1} of CDAE.

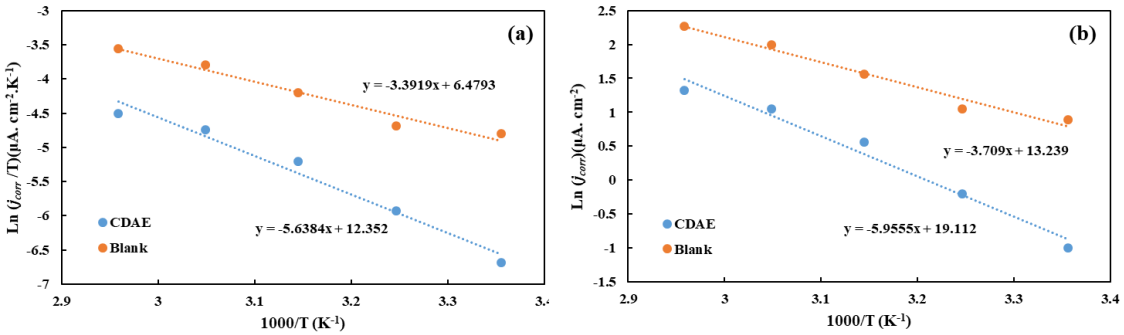

Fig. 6. Arrhenius plot (a) and Transition-state plot (b) of copper in 3.5 wt.% NaCl solution in the presence and absence of 15% v/v of CDAE.

Table 3. Polarization parameters of copper in 3.5 wt.% NaCl solution in the presence and absence of 200 mg. L^{-1} of CDAE at various temperatures.

Sample	*T*(K)	E_{corr} (mV)	j_{corr} (µA. cm^{-2})	β_a (mV. dec^{-1})	β_c (mV. dec^{-1})	*IE*%
Blank	298	-510	2.45	112.51	114.63	--
	308	-505	2.85	56.26	55.23	--
	318	-495	4.75	43.81	74.65	--
	328	-485	7.35	49.92	75.42	--
	338	-480	9.66	51.66	75.51	--
CDAE	298	-495	0.37	65.14	74.85	84.9
	308	-490	0.82	46.36	56.56	71.2
	318	-485	1.75	50.84	94.07	63.2
	328	-480	2.86	51.76	97.83	61.1
	338	-475	3.74	44.57	77.89	61.3

To determine the mechanism of corrosion inhibition on the copper surface, the activation energy (E_a) must be calculated using the Arrhenius equation (Eq. 11):

$$j_{corr} = A \,.\exp\left(\frac{-E_a}{RT}\right) \quad (11)$$

where E_a is the apparent effective activation energy, A is the Arrhenius pre-exponential factor, R is the universal

gas constant, and T is the temperature in Kelvin. To determine the E_a of copper corrosion in the presence and absence of CDAE, $ln(j_{corr})$ was plotted against 1000/T (Figure 6a), where the slope is equal to $-E_a/R$. The calculated E_a values in the presence and absence of CDAE are 47.41 and 19.42 kJ. mol^{-1}, respectively. The inhibition process predominantly occurs through physical adsorption, as the E_a values are lower than 80 kJ. mol^{-1}. Additionally, the higher E_a value observed in the presence of the inhibitor indicates a stronger adsorption of inhibitor molecules onto the copper surface. Another form of the Arrhenius equation, the transition-state equation, was utilized to obtain the thermodynamic parameters ΔH and ΔS (Eq. 12):

$$\ln \frac{j_{corr}}{T} = \left[\mathrm{Ln}\left(\frac{R}{hN_A}\right) + \left(\frac{\Delta S}{R}\right)\right] - \frac{\Delta H}{R}\left(\frac{1}{T}\right) \quad (12)$$

where h is Planck's constant ($6.6261 \times 10^{-34} j.s$) and N_a is Avogadro's number (6.0225×10^{22} molecules. mol^{-1}). To calculate ΔH and ΔS, $\mathrm{Ln}\frac{j_{corr}}{T}$ was plotted against 1000/T (Figure 6b). The slope of the linear fit is equal to $-\frac{\Delta H}{R}$ and the intercept is equal to $\left[\mathrm{Ln}\left(\frac{R}{hN_A}\right) + \left(\frac{\Delta S}{R}\right)\right]$, which yields the values for ΔH and ΔS, respectively (Table 4). The positive values of ΔH indicate that the dissolution of copper in NaCl solution is an endothermic process, regardless of the presence of CDAE. Furthermore, the increase in ΔH in the presence of the inhibitor demonstrates that the reduction of j_{corr} is primarily controlled by the kinetic parameters of activation. The increase in ΔS with the addition of the inhibitor reveals that the activated complex in the rate-determining step represents an association rather than a dissociation step, implying a decrease in disordering as the system transitions from reactants to the activated complex. To demonstrate that green corrosion inhibitors are suitable alternatives to synthetic and unnatural inhibitors, a brief comparison between CDAE and several synthetic inhibitors was conducted. The results of this comparison, listed in Table 5, clearly show that the inhibition efficiency (*IE%*) of CDAE exceeds that of most synthetic inhibitors.

Table 4. ΔH and ΔS values for copper in 3.5 wt.% NaCl solution with and without CDAE.

Sample	ΔH (J. mol^{-1})	ΔS (J. mol^{-1}. K^{-1})
Blank	28.2	-162.8
CDAE	46.9	-113.9

Conclusions

In this study, the corrosion inhibition performance of *Cynodon dactylon* aqueous extract (CDAE) on copper in a 3.5 wt.% NaCl solution was thoroughly investigated. The chemical composition of the extract, analyzed via GC-MS, identified several bioactive compounds that are likely responsible for the protective properties of the extract. Electrochemical measurements, including polarization (LSV) and impedance spectroscopy (EIS), consistently demonstrated that CDAE acts as an efficient, mixed-type corrosion inhibitor for copper. The inhibition efficiency (IE%) increased significantly with the concentration of the inhibitor, reaching a maximum value of 91.63% at 300 mg. L^{-1}. Impedance data revealed that the adsorption of CDAE molecules onto the copper surface leads to an increase in the charge transfer resistance R_{ct} and a decrease in the double layer capacitance C_{dl}, indicating the formation of a stable, protective film at the metal-electrolyte interface. Surface analysis via SEM-EDS confirmed the results obtained from electrochemical techniques, showing a substantial reduction in the corrosion-induced damage on the copper surface in the presence of the inhibitor. Temperature-dependent studies indicated that the corrosion inhibition process follows a physical adsorption mechanism, as evidenced by the activation energy E_a values. Furthermore, thermodynamic parameters ΔH and ΔS suggested that the dissolution of copper is an endothermic process and that the presence of the inhibitor effectively controls the kinetic parameters of activation. Finally, the comparison between CDAE and various synthetic inhibitors demonstrated that this green, plant-based extract is a highly effective, eco-friendly, and cost-efficient alternative for the protection of copper against corrosion in aggressive saline environments.

Declaration of competing interest

The authors declare that they have no known competing financial interests or personal relationships that could have appeared to influence the work reported in this paper.

Data availability

Data will be made available on request.

Acknowledgment

Biosensor and Energy Research Center, Ayatollah Boroujerdi University are acknowledged for financial support of this work.

Funding Sources

The authors declare that no external funding was received for this work.

References

[1] Verma, C., Ebenso , E.E., Bahadur , I., Quraishi, M.A., An overview on plant extracts as

environmental sustainable and green corrosion inhibitors for metals and alloys in aggressive corrosive media, ***Journal of Molecular Liquids*****, 2018,** 266, 577-590. https://doi.org/10.1016/j.molliq.2018.06.110

[2] Alemnezhad, M.M., Hosseini, M. Panahimehr, M., Green corrosion protection of copper in chloride media with Calystegia sepium extract using electrochemical and GC-MS/MS analyses, ***Scientific Reports*****, 2026,** 16, 11267. https://doi.org/10.1038/s41598-026-41526-y

[3] Askari, M., Ghaffarinejad, A., Alemnezhad, M.M., Green corrosion inhibition of carbon steel in HCl by Spartium junceum petals extract: Electrochemical and computational insights, ***Martials Today Communications*****, 2025,** 48, 113434. https://doi.org/10.1016/j.mtcomm.2025.113434

[4] Fekri M.H., Omidali, F., Alamnezhad M.M., Gaffarinejad, A., Turnip peel extract as green corrosion bio-inhibitor for copper in 3.5% NaCl solution, ***Martials Chemistry and Physics*****, 2022,** 286, 126150. https://doi.org/10.1016/j.matchemphys.2022.126150

[5] Gholizadeh, M.R., Ghaffarinejad, A., Alemnezhad, M.M., Plant derived corrosion inhibitor for copper: Integrated electrochemical and molecular insights into Ailanthus altissima seed extract performance in saline media, ***Next Materials***, **11**, 2026, 101621. https://doi.org/10.1016/j.nxmate.2026.101621

[6] Tahmasbi, E., Hosseini, M., Alemnezhad, M.M., Omidali, F., Shokry, S., Garavand, R., Ghamari Kargar, P., Development of a sustainable magnetized bio-nano adsorbent from tomato residues for removal of Ni (II) ion from dairy effluents: Kinetics, thermodynamics, and practical applicability, ***Next Materials***, **2026**, 11, 101770. https://doi.org/10.1016/j.nxmate.2026.101770

[7] Raja, P.B., Ismail, M., Ghoreishiamiri, S., Mirza, J., Ismail, M.C., Kakooei, S., Abdul Rahim, A., Reviews on Corrosion Inhibitors: A Short View, ***Chemical Engineering Communications***, **2016**, 203, 1145-1156. https://doi.org/10.1080/00986445.2016.1172485

[8] Finsgar, M., Jackson, J., Application of corrosion inhibitors for steels in acidic media for the oil and gas industry: A review, ***Corrosion Science***, **2014**, 86, 17-41. https://doi.org/10.1016/j.corsci.2014.04.044

[9] El Shahaly, O.M., Abdel-Rahman, A.A.H., Abd El-Sattar, N.E.A., El-sayed, H.A., Abdelshafi, N.S., Synergistic copper corrosion inhibition in 1.0 M HCl by eco-friendly heteroatom inhibitors and zinc nanomaterials: Experimental and computational study, ***Journal of Industrial and Engineering Chemistry***, **2026**, https://doi.org/10.1016/j.jiec.2026.01.038

[10] Finšgar, M., Jackson, J., Application of corrosion inhibitors for steels in acidic media for the oil and gas industry: A review, Corrosion Science, 2014, 86, 17–41, https://doi.org/10.1016/j.corsci.2014.04.044

[11] Verma, C., Ebenso, E.E., Bahadur, I., Quraishi, M.A., An overview on plant extracts as environmental sustainable and green corrosion inhibitors for metals and alloys in aggressive corrosive media, ***Journal of Molecular Liquids***, **2018**, 266, 577-590, https://doi.org/10.1016/j.molliq.2018.06.110

[12] Chauhan, D.S., Quraishi, M.A., Sorour, A.A., Saha, S.K., Banerjee, P., Triazole-modified chitosan: A biomacromolecule as a new environmentally benign corrosion inhibitor for carbon steel in a hydrochloric acid solution, ***International Journal of Biological Macromolecules*****, 2020**, 152, 399-411, https://doi.org/10.1016/j.ijbiomac.2020.02.210

[13] Lgaz, H., Salghi, R., Jodeh, S., Hammouti, B., Effect of organic corrosion inhibitors on corrosion performance of metals in aggressive media: A review, ***Journal of Molecular Liquids***, **2021**, 330, 115702, https://doi.org/10.1016/j.molliq.2021.115702

[14] Alaneme, K.K., Olusegun, S.J., Adelowo, O.T., Corrosion inhibition and adsorption mechanism

studies of Hunteria umbellata seed husk extracts on mild steel immersed in acidic solutions, ***Alexandria Engineering Journal*****, 2022**, 61(4), 2735-2746, https://doi.org/10.1016/j.aej.2021.08.038

[15] Verma, C., Ebenso, E.E., Bahadur, I., Quraishi, M.A., An overview on plant extracts as environmental sustainable and green corrosion inhibitors for metals and alloys in aggressive corrosive media, ***Journal of Molecular Liquids***, **2018**, 266, 577-590. https://doi.org/10.1016/j.molliq.2018.06.110

[16] Raja, P.B., Sethuraman, M.G., Natural products as corrosion inhibitor for metals in corrosive media-A review, ***Materials Letters***, **2008**, 62(1), 113-116. https://doi.org/10.1016/j.matlet.2007.04.07

[17] Lgaz, H., Salghi, R., Larouj, M., Jodeh, S., El Harti, M., Hammouti, B., Oukhrib, R., Adsorption and corrosion inhibition effect of naturally occurring organic molecules on carbon steel in aggressive media: A review, ***Journal of Molecular Liquids***, **2017**, 244, 154-168. https://doi.org/10.1016/j.molliq.2017.08.076

[18] Chigondo, M., Chigondo, F., Recent natural corrosion inhibitors for mild steel: An overview, ***Journal of Chemistry***, **2016**, 2016, 6208937. https://doi.org/10.1155/2016/6208937

[19] Alaneme, K.K., Olusegun, S.J., Adelowo, O.T., Corrosion inhibition and adsorption mechanism studies of Hunteria umbellata seed husk extracts on mild steel immersed in acidic solutions, ***Alexandria Engineering Journal***, **2022**, 61(4), 2735-2746. https://doi.org/10.1016/j.aej.2021.08.038

[20] Hosseini M., Castillo R., Soleymani M., A novel magnetic-assisted ionic liquid-based microextraction method (MA-ILBME): Specific design system for sensitive spectrophotometric analysis of paracetamol as a pharmaceutical pollutant in environmental samples, ***Talanta*****, 2025**, 286, 127486. https://doi.org/10.1016/j.talanta.2024.127486

[21] Hosseini, M., A high-performance ionic liquid-based microextraction (ILBME) method for the trace determination of paroxetine as a pharmaceutical pollutant in environmental and biological samples, ***Analytical Methods*****, 2024**, 16, 8457-8470. https://doi.org/10.1039/D4AY01668H

[22] Hosseini, M., Gallardo, K., A novel system based on a task-specific pyrrolinium-based ionic liquid and homogeneous in situ solvent formation microextraction for the determination of sertraline in real water and urine samples, ***New Journal of Chemistry*****, 2025,** 49, 13772-13784. https://doi.org/10.1039/D5NJ01661D

[23] Hosseini, M., Development of an ionic liquid-based microextraction system (ILBME) for sensitive spectrophotometric analysis of neodymium(III) ions in environmental samples, ***International Journal of Environmental Analytical Chemistry***, **2024**, 105, 6203-6220. https://doi.org/10.1080/03067319.2024.2414868

[24] Lei, Y., Wang, F., Li, S., Liu, J., Interfacial adsorption behavior of task-specific ionic liquids as highly efficient corrosion inhibitors for copper in chloride solution, ***Journal of Molecular Liquids*****, 2022**, 357, 119120, https://doi.org/10.1016/j.molliq.2022.119120

[25] Verma, C., Ebenso, E.E., Quraishi, M.A., Ionic liquids as green corrosion inhibitors: A review, ***Journal of Molecular Liquids***, **2017**, 233, 116-126. https://doi.org/10.1016/j.molliq.2017.03.105

[26] Bensajjay, F., Alehyen, S., Hajjaji, N., El Haji, M., Adsorption and inhibition performance of plant extracts on steel corrosion in acidic media, ***Corrosion Science*****, 2011**, 53(4), 1457-1468. https://doi.org/10.1016/j.corsci.2010.12.012

[27] Xiaoyan, L., Shuduan, D., Huaqing, F., Inhibition of mild steel corrosion in hydrochloric acid solution by hexamethylenetetramine and synergistic iodide ions, ***Corrosion Science***, **2012**, 62, 163-175. https://doi.org/10.1016/j.corsci.2012.05.008

[28] Abdel Salam, F., Mohamed K.E., Mohamed, A., Abo-Hussien, A.A., Corrosion inhibition of carbon steel by new thiophene derivatives in acid medium, ***Journal of Molecular Liquids*****, 2016**, 219, 396-404. https://doi.org/10.1016/j.molliq.2016.03.051

[29] Faiza, B., Mohamed, L., Marc, L., Thermodynamic characterization of metal dissolution and inhibitor adsorption processes, ***Corrosion Science***, **2005**, 47(12), 2915-2931. https://doi.org/10.1016/j.corsci.2005.05.034

[30] El Ibrahimi, B., Jmiai, A., Khadiri, A., Samira, E.I., Ali, G., Computational and experimental studies of corrosion inhibition by organic molecules: A review, ***Journal of Molecular Structure***, **2019**, 1189, 341-355. https://doi.org/10.1016/j.molstruc.2019.04.059

[31] Gürel, G., The use of quantum chemical methods in corrosion inhibitor studies, ***Corrosion Science*****, 2008**, 50(11), 2981-2992. https://doi.org/10.1016/j.corsci.2008.08.043

[32] Muthuraj, M., Archana, M., and Rajeswari, S., Cynodon dactylon leaf extract as an efficient eco-friendly corrosion inhibitor in acidic media: An experimental approach, ***Rasayan Journal of Chemistry***, **2022**, 15(3), 2123-2132. https://doi.org/10.31788/RJC.2022.1536671.

[33] Zulkifli, F., Haque, J., Daoudi, W., Ghazali, M.S.M., Izionworu, V.O., Al-Amiery, A.A., Berdimurodov, E., Praditya na, A., and Wan Nik, W.B., Cynodon dactylon extract as eco-friendly corrosion inhibitor epoxy coating addition for mild steel, ***International Journal of Corrosion and Scale Inhibition***, **2024**, 13(4), 2340–2353. https://doi.org/10.17675/2305-6894-2024-13-4-24.